



Cite this: *Chem. Sci.*, 2025, **16**, 20323

All publication charges for this article have been paid for by the Royal Society of Chemistry

Received 31st July 2025
Accepted 29th September 2025

DOI: 10.1039/d5sc05757d

rsc.li/chemical-science

Introduction

Mechanophores are stress-sensitive molecules that undergo specific and productive chemical transformations in response to mechanical force.¹ Force is transduced to mechanophores by covalently attached polymer chains.^{2,3} Mechanochromic mechanophores couple a colorimetric output, *i.e.*, a visible color change, with force-induced chemical reactions to function as molecular force probes. Mechanochromic mechanophores that undergo reversible color changes in response to mechanical activation enable the detection of stress and/or strain in polymeric materials and have potential applications in patterning, data storage, and damage sensing. A rich library of mechanochromic mechanophores has been developed with applications in bulk materials for stress detection including derivatives of naphthopyran,⁴ spiropyran,⁵ spirothiopyran,⁶ oxazine,⁷ diarylbibenzofuranone,^{8,9} and rhodamine.^{10,11} Our group has dedicated significant effort to the development of naphthopyran force probes, which we have identified as a privileged class of mechanochromic mechanophores due to their synthetic accessibility and structural and functional modularity.¹²

Naphthopyran mechanophores undergo a ring-opening reaction to generate highly colored merocyanine dyes in response to mechanical force.¹² Mechanochemical activation of naphthopyran derivatives has been achieved using ultrasonication in solution,^{13–16} and in bulk materials under tensile and compressive stress.^{4,13–15,17} We have been particularly interested in multimodal naphthopyran mechanophores that

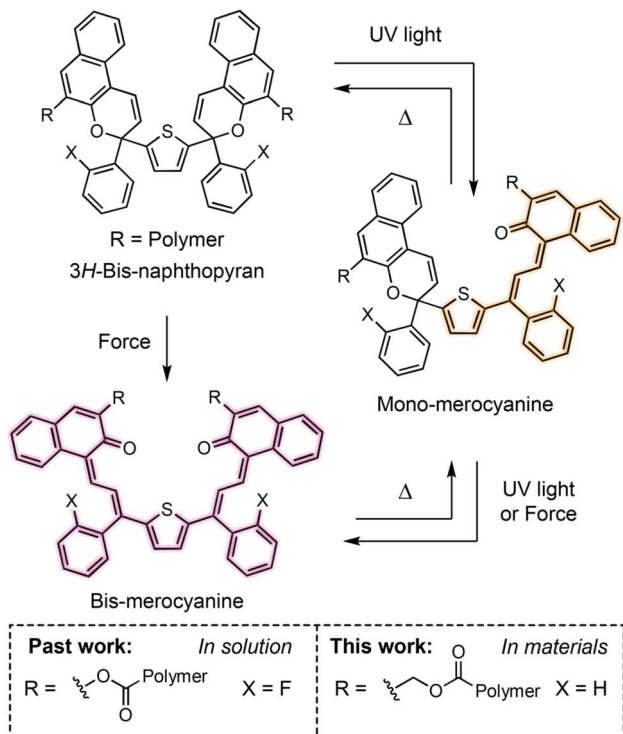
Strain-dependent multicolor mechanochromism of 3H-bis-naphthopyran in solid polymeric materials

Skylar K. Osler, Audrey V. Conner, Molly E. McFadden and Maxwell J. Robb *

Multimodal mechanophores are important targets for the design of complex stress-sensing materials due to their multicolor mechanochromic properties, which potentially enable discrete visual outputs under varying levels of stress and/or strain. We have developed a novel 3H-bis-naphthopyran mechanophore that imbues solid polymeric materials with force-dependent colorimetric sensing capabilities. Polydimethylsiloxane (PDMS) elastomers incorporating a 3H-bis-naphthopyran crosslinker were synthesized and deformed under uniaxial tension. The relative distribution of two distinctly colored merocyanine dyes is systematically biased under varying levels of applied stress and/or strain, resulting in the appearance of distinct coloration, which is characterized by pronounced changes in visible absorption spectra. This work demonstrates that judiciously designed bis-naphthopyran mechanophores can function as force sensors that visually report on the magnitude of applied force in elastomeric materials.

contain multiple pyran reactive sites, as these molecules provide access to distinct states that are coupled to unique absorption properties, and therefore visual signals.¹⁸ Multimodal bis-naphthopyran^{19,20} and naphthodipyrans²¹ mechanophores exhibit multicolor mechanochromism in solution-phase ultrasonication experiments, displaying varying coloration as a function of force or the duration of ultrasound exposure, respectively. However, multicolor mechanochromism from naphthopyran mechanophores has not been achieved to date in bulk materials. In a few examples, stress and/or strain-dependent multicolor mechanochromism has been demonstrated in bulk materials that incorporate two distinct mechanophores.^{22–25} These dual mechanophore systems typically capitalize on either the unique mechanical properties within different regions of multi-material networks or polymer blends, and/or the distinct reversion behavior of the mechanophores to achieve a multicolor response. Significantly, demonstrations of gradient multicolor mechanochromism from a single mechanophore in bulk materials are so far limited to non-covalent systems. Sommer and coworkers reported the torsional spring mechanophore, which exhibits subtle but well-defined changes in absorption wavelength as a function of applied stress.^{26,27} Mechanophores that display stress-dependent changes in fluorescence emission have also been described; however, they require irradiation with UV light for detection and are not easily observable by the naked eye.^{28–30} Polymeric materials that incorporate multimodal naphthopyrans are theoretically capable of distinguishing between varying mechanical loads through discreet visual signals and remain a highly desirable research target in the field of polymer mechanochemistry.





Scheme 1 Mechanochromic and photochromic reactivity of 3H-bis-naphthopyran mechanophores.

We previously reported a 3H-bis-naphthopyran mechanophore that combines two naphthopyran subunits linked to a central thiophene ring (Scheme 1).¹⁹ Photochemical or mechanochromic activation of this 3H-naphthopyran compound generates interconverting mono- and bis-merocyanine isomers that display yellow and purple coloration, respectively. Whereas photochemical activation with UV light promotes sequential ring-opening reactions to generate mono-merocyanine and then bis-merocyanine dyes,^{31–33} ultrasound-induced mechanochromic activation results in the generation of the purple-colored bis-merocyanine dye directly from the fully ring-closed bis-naphthopyran.¹⁹ Under these conditions, the yellow-colored mono-merocyanine product is generated exclusively from the thermal cycloreversion of the bis-merocyanine. Force-dependent multicolor mechanochromism in solution is achieved *via* a dynamic equilibrium that is established by the relative rates of force-induced ring-opening and thermal cycloreversion; the position of this equilibrium depends on the magnitude of force applied to the mechanophore, which is dictated by the length of the attached polymer chain.^{19,34} Unfortunately, incorporating this particular bis-naphthopyran mechanophore into bulk materials results in significant background coloration and has impeded research toward successful solid-state applications in our laboratory.

Results and discussion

Here, we report a novel 3H-bis-naphthopyran mechanophore that achieves force-dependent multicolor mechanochromism in

crosslinked polydimethylsiloxane (PDMS) elastomers subjected to varying loads under uniaxial tension. Key to this advance is the judicious incorporation of structural features on the 3H-bis-naphthopyran scaffold that increase the force-free rate of cycloreversion from the merocyanine states. In direct contrast, our previously studied bis-naphthopyran mechanophore incorporated substituents, including *ortho*-fluoro groups and aryl ester linkages, designed to increase the lifetime of the merocyanine species and enhance their accumulation in solution.^{19,32,35} Eliminating the *ortho*-fluoro substituents and incorporating a methylene spacer at the polymer attachment position on the naphthopyran core significantly reduces undesired background coloration in PDMS materials (see Scheme 1).¹⁷ Enabled by these structural modifications, we hypothesized that increasing tension applied to a polymer network incorporating 3H-bis-naphthopyran crosslinks would systematically bias the mechanostationary state³⁶ comprising different concentrations of the two uniquely colored merocyanine products. While individual strands in bulk networks experience a distribution of forces due to network inhomogeneity,³⁷ the fraction of strands experiencing greater force is anticipated to increase as a function of increasing tensile load. Therefore, for an elastomer that incorporates 3H-bis-naphthopyran crosslinkers, we expect to observe a product distribution that favors the yellow-colored mono-merocyanine product at low strain values and the purple-colored bis-merocyanine species as applied tension is increased, resulting in an overall graded change in appearance from yellow to purple.

To assess the mechanochromic reactivity of the novel 3H-bis-naphthopyran compound, we performed preliminary density functional theory (DFT) calculations using the constrained geometries simulate external force (CoGEF) method^{38,39} on a truncated model at the B3LYP/6-31G* level of theory (Fig. 1). The 3H-bis-naphthopyran molecule is predicted to undergo a single ring-opening reaction to generate the mono-merocyanine product at a maximum rupture force (F_{\max}) of 4.2 nN. Further mechanical elongation is predicted to facilitate the second ring-opening reaction at a rupture force of 4.5 nN to generate the bis-merocyanine product. While data for the (R,S) diastereomer are shown in Fig. 1, the (S,S) diastereomer is also predicted to undergo similar sequential ring-opening reactions (Fig. S1). The calculated F_{\max} values, which provide a relative measure of the force sensitivity of a mechanophore,³⁸ are comparable to the F_{\max} values calculated for our previously studied 3H-bis-naphthopyran mechanophore.¹⁹

We initially performed solution phase photoirradiation experiments to understand the absorption changes that accompany the ring-opening reactions of the novel 3H-bis-naphthopyran mechanophore. With the ultimate goal of incorporating the mechanophore into PDMS elastomers *via* standard hydrosilylation chemistry (*vide infra*),⁴⁰ we synthesized small molecule 3H-bis-naphthopyran crosslinker **BNP** functionalized with terminal vinyl groups (Fig. 2a). A solution of **BNP** (8 $\mu\text{g mL}^{-1}$ in THF, 30 mM BHT) was irradiated with UV light ($\lambda = 311\text{ nm}$) for 15 min at $-78\text{ }^\circ\text{C}$ and ultraviolet-visible (UV-vis) absorption spectra were acquired using a spectrometer equipped with a cryostat to characterize merocyanine accumulation



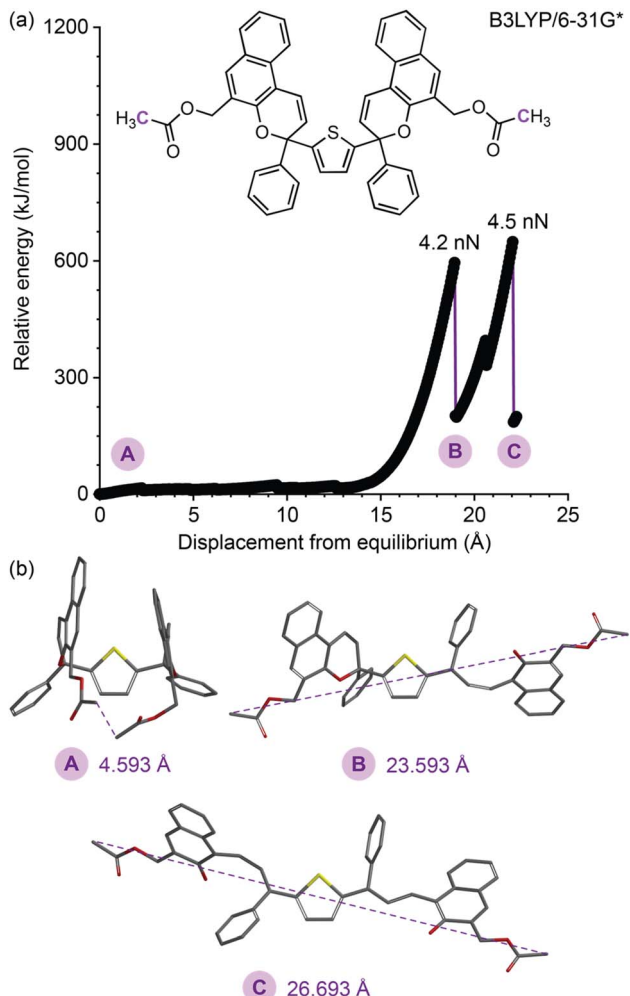


Fig. 1 (a) Density functional theory (DFT) calculations using the constrained geometries simulate external force (CoGEF) method performed on a truncated model of the 3H-bis-naphthopyran mechanophore predict the expected ring-opening reactions to generate mono-merocyanine and bis-merocyanine products. Calculations were performed at the B3LYP/6-31G* level of theory. (b) The corresponding computed structures of the truncated molecule at various points of elongation are shown along with the associated constraint distance between the terminal carbon atoms. Data for the (R,S) diastereomer shown (see the SI for additional information).

(Fig. 2b, see the SI for details). The results are consistent with previous studies that demonstrate sequential ring-opening reactions under UV light for bis-naphthopyran derivatives.^{19,31–33} At early irradiation times, the absorption spectrum is dominated by a feature with an absorption maximum at \sim 480 nm, consistent with the initial generation of the yellow-colored mono-merocyanine species. Extended photoirradiation causes the accumulated mono-merocyanine to undergo a second ring-opening reaction to generate the bis-merocyanine product, which is accompanied by a bathochromic expansion in the absorption spectrum and the emergence of an optical feature with an absorption maximum at \sim 560 nm, consistent with the extended conjugation of the bis-merocyanine dye. To provide additional insight into the

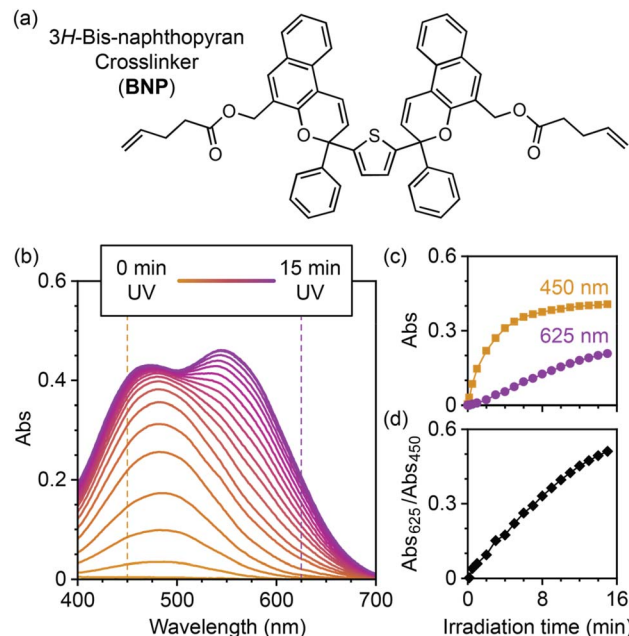


Fig. 2 (a) Structure of the 3H-bis-naphthopyran crosslinker (BNP) used in this study. (b) UV-vis absorption spectra acquired during the photoirradiation (311 nm, 15 min) of a solution of BNP in THF (8 μ g mL^{-1} , 30 mM BHT, -78 °C). (c) Absorbance at 450 nm and 625 nm as a function of photoirradiation time. (d) Ratio of the absorbance at 625 nm and 450 nm as a function of photoirradiation time.

relative rates of mono- and bis-merocyanine formation, the absorbance at characteristic wavelengths of 450 nm and 625 nm was monitored over the course of the photoirradiation experiment (Fig. 2c). Monitoring at 625 nm allows for the selective detection of the bis-merocyanine species. The absorbance at 450 nm increases rapidly at early irradiation times and approaches a plateau, while the absorbance at 625 nm increases slowly early in the experiment and then steadily increases during prolonged exposure to UV light. Importantly, the ratio of absorbance values at 625 nm and 450 nm increases over the duration of the photoirradiation experiment, reflecting the changing distribution of mono- and bis-merocyanine products (Fig. 2d). We note that the photochemically generated mono-merocyanine and bis-merocyanine dyes are stable at -78 °C in solution; however, thermal reversion is observed at 20 °C (Fig. S2). Photoirradiation of BNP at 20 °C does not result in the accumulation of any significant amount of the bis-merocyanine dye, presumably due to rapid thermal reversion at elevated temperatures (Fig. S3).³²

To investigate the mechanochemical reactivity of the 3H-bis-naphthopyran mechanophore in bulk materials, we incorporated BNP (\sim 0.8 wt% loading) into PDMS elastomers *via* Pt-catalyzed hydrosilylation⁴⁰ to yield BNP-PDMS. Uniaxial tension was applied to samples of BNP-PDMS using a load frame while in-line UV-vis absorption measurements were recorded to monitor the strain-dependent changes in absorption (Fig. 3a, see SI for details). The absorbance values at 450 nm and 625 nm were monitored during tensile experiments to investigate how the relative populations of mono-merocyanine

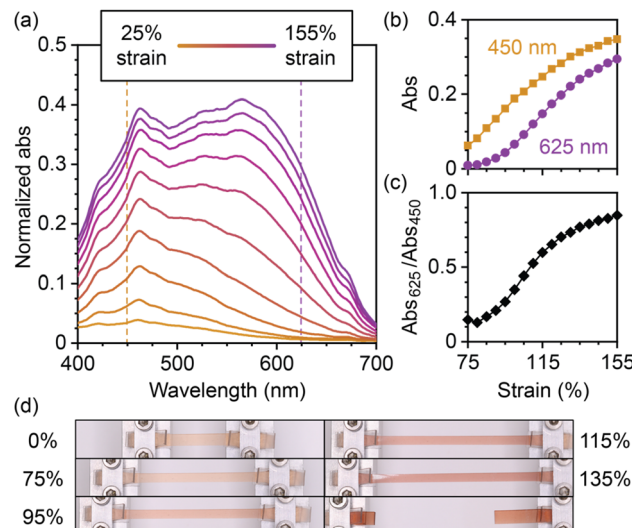


Fig. 3 (a) Normalized UV-vis absorption spectra acquired during uniaxial tensile loading of **BNP-PDMS**. (b) Absorbance at 450 nm and 625 nm as a function of strain. (c) Ratio of the absorbance at 625 nm versus 450 nm as a function of strain. (d) Photographs of a separate sample of **BNP-PDMS** at various strain values. The sample failed between 135 and 140% strain.

and bis-merocyanine products vary as a function of mechanical loading (Fig. 3b). At low strain values, the absorption spectrum is dominated by shorter wavelength features (400–550 nm), consistent with a merocyanine population that is enriched in the yellow-colored mono-merocyanine species. As the strain is increased, absorption at longer wavelengths (>550 nm) increases monotonically, indicating that the bis-merocyanine species is accumulating at increasing concentrations with higher mechanical loading. The relative population of merocyanine species is increasingly biased toward the bis-merocyanine product at higher strain values, which is reflected in the ratio of the absorbance values at 625 nm and 450 nm over the course of the tensile loading experiment (Fig. 3c). Photographs of a separate sample of **BNP-PDMS** that was subjected to identical uniaxial tensile loading illustrate the force-dependent variation in color that results from the varying composition of merocyanine species at discrete strain values (Fig. 3d and S4). We note that these results do not necessarily distinguish between two potential activation pathways whereby the bis-merocyanine species is generated either directly from the bis-naphthopyran mechanophore, or by the mechanochemical activation of intermediate mono-merocyanine species in a stepwise process. Ongoing work in our group is focused on understanding the mechanism of activation of multimodal naphthopyran mechanophores.

The reproducibility of the strain-dependent multicolor mechanochromic response of PDMS elastomers incorporating the 3H-bis-naphthopyran mechanophore was investigated by performing similar tensile loading experiments on three separate samples of **BNP-PDMS** (Fig. S5). In each case, increasing strain is accompanied by a bathochromic expansion in the overall absorption spectrum. Accumulation of the yellow-

colored mono-merocyanine product is consistently favored at low strain, whereas increasing concentration of the purple-colored merocyanine dye is observed with increasing tensile loading. We also performed replicate tensile loading experiments on a single sample to investigate the repeatability of the force-sensing performance. A specimen of **BNP-PDMS** was subjected to uniaxial tension to a strain of 120% and then allowed to relax in the dark for 1 h. The sample was then subjected to a second tensile loading, which revealed nearly identical changes in absorption as a function of strain (Fig. S5). Together, these results demonstrate that elastomers incorporating the 3H-bis-naphthopyran molecular force sensor exhibit reproducible and repeatable changes in color in response to varying mechanical loads. To confirm the mechanical origin of the observed behavior, a control PDMS network (**Control-PDMS**) incorporating a 3H-bis-naphthopyran mechanophore functionalized with a single terminal alkene group (~ 0.8 wt% loading) was synthesized and subjected to uniaxial tension (see SI for details). As expected, deformation of **Control-PDMS** under uniaxial tension does not result in any strain-dependent changes in color; critically, the ratio of absorbance at 625 nm and 450 nm remains constant over the course of the tensile loading experiment (Fig. S6 and S7). This result demonstrates that the generation of mono- and bis-merocyanine dyes observed upon tensile loading of **BNP-PDMS** requires force to be transduced across the 3H-bis-naphthopyran crosslinkers.

To further interrogate the multicolor mechanochromic behavior of the bis-naphthopyran mechanophore, a sample of **BNP-PDMS** was loaded to a constant strain and absorption spectra were recorded continuously to characterize the time-dependent changes in merocyanine distribution (Fig. S8). The specimen was first loaded to 90% strain and held in tension for 1 h. An increase in the overall visible absorption is observed during this period at constant strain; the ratio of the absorbance at 625 and 450 nm increases asymptotically to approach a constant value, consistent with an enrichment in the relative population of the bis-merocyanine species. Upon further increasing the strain of the sample to 120%, a similar increase in absorption is observed with the ratio of the absorbance at 625 and 450 nm again increasing to achieve a new plateau value, suggesting another shift in the equilibrium to favor additional accumulation of the bis-merocyanine species. Merocyanine reversion is not observed to any significant extent while the specimen is maintained in tension, even upon photoirradiation with white light, which is routinely used to facilitate the reversion of naphthopyran-derived merocyanine dyes (Fig. S9).¹² The mechanochemical activation of bis-naphthopyran in bulk materials therefore contrasts the previously observed solution-phase behavior, wherein ultrasound-induced mechanical activation of bis-naphthopyran rapidly establishes a dynamic equilibrium between mono- and bis-merocyanine products that results from competing rates of bis-merocyanine formation and thermal reversion.¹⁹ Notably, attenuation of the absorption spectrum occurs rapidly after a sample of **BNP-PDMS** maintained at 90% strain is relaxed to its original length, reflecting the transience of the merocyanine products in the absence of an applied force of tension (Fig. S10).



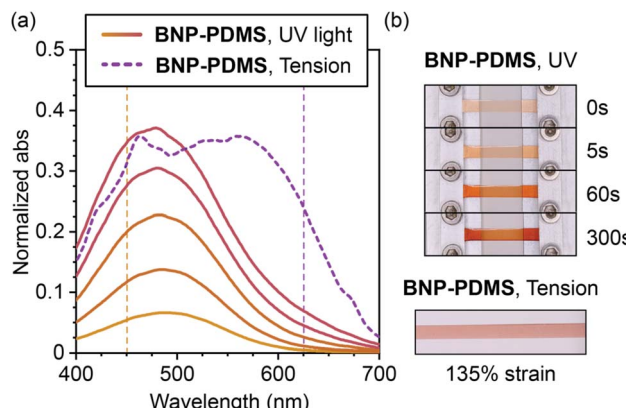


Fig. 4 (a) Absorption spectra of BNP-PDMS after 5 s, 30 s, 60 s, 120 s, and 300 s of photoirradiation with 311 nm UV light compared to a sample of BNP-PDMS at 135% strain. (b) Photographs of BNP-PDMS after 0 s, 5 s, 60 s, and 300 s of photoirradiation with UV light compared to a sample of BNP-PDMS at 135% strain.

Similar to the solution-phase results presented earlier, the differences between the photochemical and mechanochemical reactivity of the 3H-bis-naphthopyran mechanophore are readily apparent in PDMS materials. A sample of **BNP-PDMS** was irradiated with UV light ($\lambda = 311$ nm) for 300 s at room temperature and absorption spectra were acquired to monitor merocyanine accumulation (Fig. 4a). The absorption spectrum is dominated by a peak with a maximum at ~ 480 nm that increases in intensity with longer exposure to UV light, indicating that the distribution of photochemically generated merocyanine species strongly favors the mono-merocyanine product. Photoirradiation does not result in any significant accumulation of the bis-merocyanine product due to fast thermal reversion at room temperature, even in the solid state.^{19,32} We note that photodegradation and an overall decrease in visible absorption was observed upon extended UV photoirradiation (Fig. S11). The photochromic behavior of **BNP-PDMS** contrasts strongly with the mechanochromic properties of the material, which exhibits significant absorption at wavelengths up to ~ 700 nm upon mechanical loading to 135% strain. These differences in the merocyanine dye composition generated with either UV light or mechanical loading are readily observable by the naked eye (Fig. 4b). Samples of **BNP-PDMS** appear red-orange in color after exposure to UV light, whereas **BNP-PDMS** samples loaded in tension appear purple-red, consistent with the longer wavelength absorption observed spectroscopically that accompanies bis-merocyanine formation.

Conclusions

In summary, we have developed a novel multimodal 3H-bis-naphthopyran mechanophore that displays force-dependent multicolor mechanochromic behavior in bulk polymeric materials. Polydimethylsiloxane (PDMS) elastomers incorporating a judiciously designed 3H-bis-naphthopyran mechanophore as a crosslinker were subjected to uniaxial tensile loading and the mechanochromic properties were characterized by UV-vis

absorption spectroscopy as a function of strain. A significant bathochromic shift in the overall absorption is observed upon increasing strain applied to the materials as a result of force-dependent variation in the accumulative distribution of distinctly colored merocyanine products. At low strain, the product distribution is dominated by the yellow-colored mono-merocyanine species, while higher strains increasingly bias the population toward the purple-colored bis-merocyanine species. The strain-dependent changes in color are clearly observed in the gauge region of the PDMS elastomers at varying levels of mechanical loading. This study introduces a bis-naphthopyran mechanophore that functions as a molecular force sensor that is capable of distinguishing between different magnitudes of force through discreet colorimetric signals in solid polymeric materials.

Author contributions

M. J. R., M. E. M., and S. K. O. conceptualized the project. S. K. O. designed the research. S. K. O. and A. V. C. performed the experiments. S. K. O. and M. J. R. analyzed the data. S. K. O. and M. J. R. wrote the manuscript. M. J. R. provided guidance during all stages of the project.

Conflicts of interest

There are no conflicts to declare.

Data availability

All data are available in this published article and its supplementary information (SI). Supplementary information is available. See DOI: <https://doi.org/10.1039/d5sc05757d>.

Acknowledgements

Financial support from an NSF CAREER award (CHE-2145791) is gratefully acknowledged. We thank the Center for Catalysis and Chemical Synthesis of the Beckman Institute at Caltech for access to equipment. We thank the Peters laboratory at Caltech for use of their UV-vis spectrometer. M. J. R. gratefully acknowledges the Alfred P. Sloan Foundation for a Sloan Research Fellowship and the Camille and Henry Dreyfus Foundation for a Camille Dreyfus Teacher-Scholar Award.

References

- 1 J. Li, C. Nagamani and J. S. Moore, *Acc. Chem. Res.*, 2015, **48**, 2181–2190.
- 2 M. K. Beyer and H. Clausen-Schaumann, *Chem. Rev.*, 2005, **105**, 2921–2948.
- 3 M. M. Caruso, D. A. Davis, Q. Shen, S. A. Odom, N. R. Sottos, S. R. White and J. S. Moore, *Chem. Rev.*, 2009, **109**, 5755–5798.
- 4 M. J. Robb, T. A. Kim, A. J. Halmes, S. R. White, N. R. Sottos and J. S. Moore, *J. Am. Chem. Soc.*, 2016, **138**, 12328–12331.



5 D. A. Davis, A. Hamilton, J. Yang, L. D. Cremar, D. Van Gough, S. L. Potisek, M. T. Ong, P. V. Braun, T. J. Martínez, S. R. White, J. S. Moore and N. R. Sottos, *Nature*, 2009, **459**, 68–72.

6 H. Zhang, F. Gao, X. Cao, Y. Li, Y. Xu, W. Weng and R. Boulatov, *Angew. Chem., Int. Ed.*, 2016, **55**, 3040–3044.

7 H. Qian, N. S. Purwanto, D. G. Ivanoff, A. J. Halmes, N. R. Sottos and J. S. Moore, *Chem.*, 2021, **7**, 1080–1091.

8 K. Imato, T. Kanehara, T. Ohishi, M. Nishihara, H. Yajima, M. Ito, A. Takahara and H. Otsuka, *ACS Macro Lett.*, 2015, **4**, 1307–1311.

9 K. Imato, A. Irie, T. Kosuge, T. Ohishi, M. Nishihara, A. Takahara and H. Otsuka, *Angew. Chem., Int. Ed.*, 2015, **54**, 6168–6172.

10 Z. Wang, Z. Ma, Y. Wang, Z. Xu, Y. Luo, Y. Wei and X. Jia, *Adv. Mater.*, 2015, **27**, 6469–6474.

11 T. Wang, N. Zhang, J. Dai, Z. Li, W. Bai and R. Bai, *ACS Appl. Mater. Interfaces*, 2017, **9**, 11874–11881.

12 M. E. McFadden, R. W. Barber, A. C. Overholts and M. J. Robb, *Chem. Sci.*, 2023, **14**, 10041–10067.

13 M. E. McFadden and M. J. Robb, *J. Am. Chem. Soc.*, 2021, **143**, 7925–7929.

14 S. K. Osler, M. E. McFadden and M. J. Robb, *J. Polym. Sci.*, 2021, **59**, 2537–2544.

15 Y. Sun, M. E. McFadden, S. K. Osler, R. W. Barber and M. J. Robb, *Chem. Sci.*, 2023, **14**, 10494–10499.

16 S. K. Osler, N. A. Ballinger and M. J. Robb, *J. Am. Chem. Soc.*, 2025, **147**, 3904–3911.

17 B. A. Versaw, M. E. McFadden, C. C. Husic and M. J. Robb, *Chem. Sci.*, 2020, **11**, 4525–4530.

18 D. Kim, M. S. Kwon and C. W. Lee, *Polym. Chem.*, 2022, **13**, 5177–5187.

19 M. E. McFadden and M. J. Robb, *J. Am. Chem. Soc.*, 2019, **141**, 11388–11392.

20 S. K. Osler, M. E. McFadden, T. Zeng and M. J. Robb, *Polym. Chem.*, 2023, **14**, 2717–2723.

21 M. E. McFadden, S. K. Osler, Y. Sun and M. J. Robb, *J. Am. Chem. Soc.*, 2022, **144**, 22391–22396.

22 T. Kosuge, X. Zhu, V. M. Lau, D. Aoki, T. J. Martinez, J. S. Moore and H. Otsuka, *J. Am. Chem. Soc.*, 2019, **141**, 1898–1902.

23 K. Ishizuki, D. Aoki and H. Otsuka, *Macromol. Rapid Commun.*, 2021, **42**, 2000429.

24 T. Wang, H. Wang, L. Shen and N. Zhang, *Polym. Chem.*, 2021, **12**, 3832–3841.

25 K. Ishizuki, A. Takahashi and H. Otsuka, *Macromol. Rapid Commun.*, 2025, **46**, 2400812.

26 M. Raisch, W. Maftuhin, M. Walter and M. Sommer, *Nat. Commun.*, 2021, **12**, 4243.

27 R. Hertel, W. Maftuhin, M. Walter and M. Sommer, *J. Am. Chem. Soc.*, 2022, **144**, 21897–21907.

28 R. Kotani, S. Yokoyama, S. Nobusue, S. Yamaguchi, A. Osuka, H. Yabu and S. Saito, *Nat. Commun.*, 2022, **13**, 303.

29 T. Yamakado and S. Saito, *J. Am. Chem. Soc.*, 2022, **144**, 2804–2815.

30 H. Hu, X. Cheng, Z. Ma, R. P. Sijbesma and Z. Ma, *J. Am. Chem. Soc.*, 2022, **144**, 9971–9979.

31 W. Zhao and E. M. Carreira, *J. Am. Chem. Soc.*, 2002, **124**, 1582–1583.

32 W. Zhao and E. M. Carreira, *Chem. Eur. J.*, 2007, **13**, 2671–2685.

33 X. Lu, Q. Dong, X. Dong and W. Zhao, *Tetrahedron*, 2015, **71**, 4061–4069.

34 P. A. May, N. F. Munaretto, M. B. Hamoy, M. J. Robb and J. S. Moore, *ACS Macro Lett.*, 2016, **5**, 177–180.

35 B. Van Gemert, in *Organic Photochromic and Thermochromic Compounds*, Springer, Boston, MA, 2002, pp. 111–140.

36 C. K. Lee, D. A. Davis, S. R. White, J. S. Moore, N. R. Sottos and P. V. Braun, *J. Am. Chem. Soc.*, 2010, **132**, 16107–16111.

37 E. M. Lloyd, J. R. Vakil, Y. Yao, N. R. Sottos and S. L. Craig, *J. Am. Chem. Soc.*, 2023, **145**, 751–768.

38 I. M. Klein, C. C. Husic, D. P. Kovács, N. J. Choquette and M. J. Robb, *J. Am. Chem. Soc.*, 2020, **142**, 16364–16381.

39 M. K. Beyer, *J. Chem. Phys.*, 2000, **112**, 7307–7312.

40 G. R. Gossweiler, G. B. Hewage, G. Soriano, Q. Wang, G. W. Welshofer, X. Zhao and S. L. Craig, *ACS Macro Lett.*, 2014, **3**, 216–219.

